Published OnlineFirst July 11, 2018; DOI: 10.1158/0008-5472.CAN-17-3822

Tumor Biology and Immunology

Cancer Research

Altered Cell-Cycle Control, Inflammation, and Adhesion in High-Risk Persistent Bronchial Dysplasia

Daniel T. Merrick[1], Michael G. Edwards[2], Wilbur A. Franklin[1], Michio Sugita[1], Robert L. Keith[3,4], York E. Miller[3,4], Micah B. Friedman[1], Lori D. Dwyer-Nield[3,5], Meredith A. Tennis[4], Mary C. O'Keefe[6], Elizabeth J. Donald[1], Jessica M. Malloy[1], Adrie van Bokhoven[1], Storey Wilson[1], Peter J. Koch[7], Charlene O'Shea[7], Christopher Coldren[8], David J. Orlicky[1], Xian Lu[9], Anna E. Baron[9], Greg Hickey[4], Timothy C. Kennedy[4], Roger Powell[5], Lynn Heasley[10], Paul A. Bunn[11], Mark Geraci[12], and Raphael A. Nemenoff[4,13]

Abstract

Persistent bronchial dysplasia is associated with increased risk of developing invasive squamous cell carcinoma (SCC) of the lung. In this study, we hypothesized that differences in gene expression profiles between persistent and regressive bronchial dysplasia would identify cellular processes that underlie progression to SCC. RNA expression arrays comparing baseline biopsies from 32 bronchial sites that persisted/progressed to 31 regressive sites showed 395 differentially expressed genes [ANOVA, FDR $\leq$ 0.05). Thirty-one pathways showed significantly altered activity between the two groups, many of which were associated with cell-cycle control and proliferation, inflammation, or epithelial differentiation/cell–cell adhesion. Cultured persistent bronchial dysplasia cells exhibited increased expression of Polo-like kinase 1 (PLK1), which was associated with multiple cell-cycle pathways. Treatment with PLK1 inhibitor induced apoptosis and G_2–M arrest and decreased proliferation compared with untreated cells; these effects were not seen in normal or regressive bronchial dysplasia cultures. Inflammatory pathway activity was decreased in persistent bronchial dysplasia, and the presence of an inflammatory infiltrate was more common in regressive bronchial dysplasia. Regressive bronchial dysplasia was also associated with trends toward overall increases in macrophages and T lymphocytes and altered polarization of these inflammatory cell subsets. Increased desmoglein 3 and plakoglobin expression was associated with higher grade and persistence of bronchial dysplasia. These results identify alterations in the persistent subset of bronchial dysplasia that are associated with high risk for progression to invasive SCC. These alterations may serve as strong markers of risk and as effective targets for lung cancer prevention.

Significance: Gene expression profiling of high-risk persistent bronchial dysplasia reveals changes in cell-cycle control, inflammatory activity, and epithelial differentiation/cell–cell adhesion that may underlie progression to invasive SCC. *Cancer Res; 78(17); 4971–83. ©2018 AACR.*

Introduction

Mortality associated with non–small cell lung cancer (NSCLC) is higher than the next four tumor types combined and will claim the lives of more than 160,000 people in the United States this year (1, 2). Early detection via screening with low-dose CT (LDCT) has contributed to improved survival (3, 4), but is most effective for detection of peripheral tumors that are predominantly of the adenocarcinoma subtype. LDCT does not detect bronchial dysplasia, the precursor of invasive squamous cell carcinoma (SCC). Bronchial dysplasia arises in the central airways of the lung and

[1]Department of Pathology, University of Colorado Anschutz Medical Campus, Aurora, Colorado. [2]Department of Medicine/Division of Pulmonary Medicine, University of Colorado Anschutz Medical Campus, Aurora, Colorado. [3]Department of Medicine/Division of Pulmonary Medicine, Denver Veterans Affairs Medical Center, Aurora, Colorado. [4]Department of Medicine/Division of Pulmonary Medicine, University of Colorado Anschutz Medical Campus, Aurora, Colorado. [5]School of Pharmacy, University of Colorado Anschutz Medical Campus, Aurora, Colorado. [6]Department of Pathology, Denver Health Medical Center, Denver, Colorado. [7]Department of Regenerative Medicine and Stem Cell Research, University of Colorado Anschutz Medical Campus, Aurora, Colorado. [8]PathGroup LLC, Nashville, Tennessee. [9]Department of Biostatistics and Informatics, Colorado School of Public Health, Denver, Colorado. [10]Department of Craniofacial Biology, University of Colorado Anschutz Medical Campus, Aurora, Colorado. [11]Department of Medicine/Division of Medical Oncology, University of Colorado Anschutz Medical Campus, Aurora, Colorado. [12]Department of Medicine, Indiana University, Bloomington, Indiana. [13]Department of Medicine, Division of Renal Medicine, University of Colorado Anschutz Medical Campus, Aurora, Colorado.

Note: Supplementary data for this article are available at Cancer Research Online (http://cancerres.aacrjournals.org/).

Corresponding Author: Daniel T. Merrick, University of Colorado School of Medicine, Mail Stop 8104, 12801 E 17th Avenue, Room 5114, Aurora, CO 80045. Phone: 303-724-4321; Fax: 303-724-3096; E-mail: Dan.Merrick@ucdenver.edu

doi: 10.1158/0008-5472.CAN-17-3822

Published OnlineFirst July 11, 2018; DOI: 10.1158/0008-5472.CAN-17-3822

can be detected by bronchoscopic means especially when advanced techniques such as autofluorescence, narrow-band imaging, and other recently developed technologies are employed (5, 6). When present, these lesions represent a stage in the development of invasive lung cancer at which application of preventive measures in secondary (patients without a history of lung cancer) or tertiary (patients with a history of lung cancer) settings could be utilized to significantly reduce lung cancer–associated mortality.

The relationship between bronchial dysplasia and SCC is well established with the demonstration of increased risk when higher grades of bronchial dysplasia are present and the description of molecular alterations in bronchial dysplasia that parallel those seen in invasive SCC (7–13). However, the large majority of bronchial dysplasias, including high-grade lesions (moderate dysplasia or worse), do not progress to invasive SCC (14–16). We have recently shown that patients harboring multiple sites within the airways that persist as or progress to high-grade dysplasia represent a subset of patients with aggressive airway disease that have a 7.8-fold increase in risk for the development of SCC (17).

We hypothesize that changes in gene expression that distinguish high risk persistent from low risk regressive bronchial dysplasia will elucidate key cellular activities that mediate progression of premalignant lesions to invasive SCC. Cellular processes associated with persistence are further explored to demonstrate a potential role in mediating malignant progression. The description of these gene expression alterations will provide information that can be used to predict risk associated with bronchial dysplasia and identify targets for prevention of progression to invasive SCC.

Materials and Methods

Subject and biopsy characteristics

All tissues used in these studies were obtained from subjects who directly or through their guardians signed informed written consents for these types of analyses. These tissues were collected via Colorado SPORE in Lung Cancer bronchoscopy protocols that were approved by the Colorado Multiple Institutional Review Board (CoMIRB). CoMIRB and University of Colorado investigators follow the policies of the U.S. Common Rule. Biopsies from the treatment arm of the iloprost chemoprevention trial were excluded as this trial demonstrated a reduction in outcome histology related to iloprost treatment in former smokers (18). Inclusion criteria consisted of availability of snap-frozen biopsy tissue from a site with a known baseline histology as defined from the adjacent formalin-fixed, paraffin-embedded (FFPE) biopsy, and a known outcome histology as defined in FFPE biopsy at the same bronchial site on a subsequent bronchoscopy (mean time to follow-up biopsy, 12.3 months, see Supplementary Table S1). Autofluorescence bronchoscopy was used to initially identify dysplastic lesions in the airways. Follow-up biopsy sites were determined by reviewing prior images using a common map and algorithm of sequential appearance and orientation of orifices in the airways in protocols developed and employed by bronchoscopists with over 25 years of experience (R.L. Keith, Y.E. Miller, and T.C. Kennedy). Histology was scored using a system in which numeric assignments were given for each level of atypia as reported previously (see Fig. 1; ref. 17). Inflammation scores generated during microscopic assessment of hematoxylin and eosin (H&E)–stained biopsy slides indicate overall cellularity attributed to inflammatory cells as normal (<5%), mild (5%–25%), moderate (25%–75%), and severe (>75%). Where possible, specimens in test groups were selected to maintain similarity in respect to baseline histology, age, gender, tobacco history, and history of NSCLC. Frozen sections were performed on the tissue used for RNA isolation and inclusion required histology that was within one diagnostic score of the adjacent FFPE section (frozen diagnoses were assigned to a site when there was a one score difference). A total of 200 ng of total RNA and RNA integrity number (RIN; Agilent Bioanalyzer) of 2.5 or higher were also required for inclusion. Consistency of overall gene expression levels within groups were evaluated to confirm that differences in RIN did not significantly correlate with differences in gene expression levels. Sixty-three of 107 processed frozen biopsies met criteria for inclusion with 21 excluded for discordant histology and 23 for inadequate RNA quality/quantity. Cultures of primary, unimmortalized bronchial epithelial cells were selected from Colorado SPORE in Lung Cancer tissue bank stores of cultures previously established from fresh biopsy tissue. Because frozen and fresh biopsies were collected only from selected sites at bronchoscopy (usually one or two sites per bronchoscopy), all but three cultures were from sites other than those included in the gene expression analysis. Cultures were classified as persistent or regressive dysplasia based on diagnoses from concurrent immediately adjacent and subsequent FFPE biopsies at the same site.

Gene expression microarray analysis

Baseline histologic scores (HS) of 4 or higher were considered dysplasia and less than or equal to 2 considered nondysplasia. Processing of biopsies for gene expression analysis was performed with simultaneous evaluation by H&E-stained frozen sections. Biopsies frozen in optimal cutting tissue solution (OCT; Fisher Healthcare) at collection and stored in liquid nitrogen were placed in a cryostat at −25°C and mounted *in toto* for sectioning. A superficial section was assessed by H&E stain and if demonstrating the appropriate histology, tissue was removed from the cryostat chuck in a manner to prevent thawing and immediately placed in RNeasy (Qiagen). RNA was extracted within 60 minutes and resuspended in 12 μL of RNAse free water. One microliter was used for bioanalyzer assessment. If the initial H&E section did not show expected histology, deeper sections were taken until the expected histology was identified or until the tissue was exhausted. Labeled RNA was hybridized with the Affymetrix Hu 1.0 array and expression levels measured by address specific signal intensity (GEO accession number: GSE114489). Gene expression data were analyzed by classification of biopsy source in two ways, firstly according to outcome histology and secondly by degree of dysplastic change in the baseline biopsy without consideration of outcome.

Culture-based PLK1 expression, apoptosis, and cell-cycle analyses

Bronchial epithelial cultures were established as described previously (19). Stocks of cells frozen at 3 to 6 weeks after primary isolation were thawed as passage 3 cultures. All experiments were performed on passage 4 to 6 cultures, and senescence was seen with all cell lines between passages 7 and 10. Identity of selected cell lines used for extended analyses was confirmed by standard STR (short tandem repeat) testing of cultured cells and associated peripheral blood collected from patients at enrollment. Whole-

Published OnlineFirst July 11, 2018; DOI: 10.1158/0008-5472.CAN-17-3822

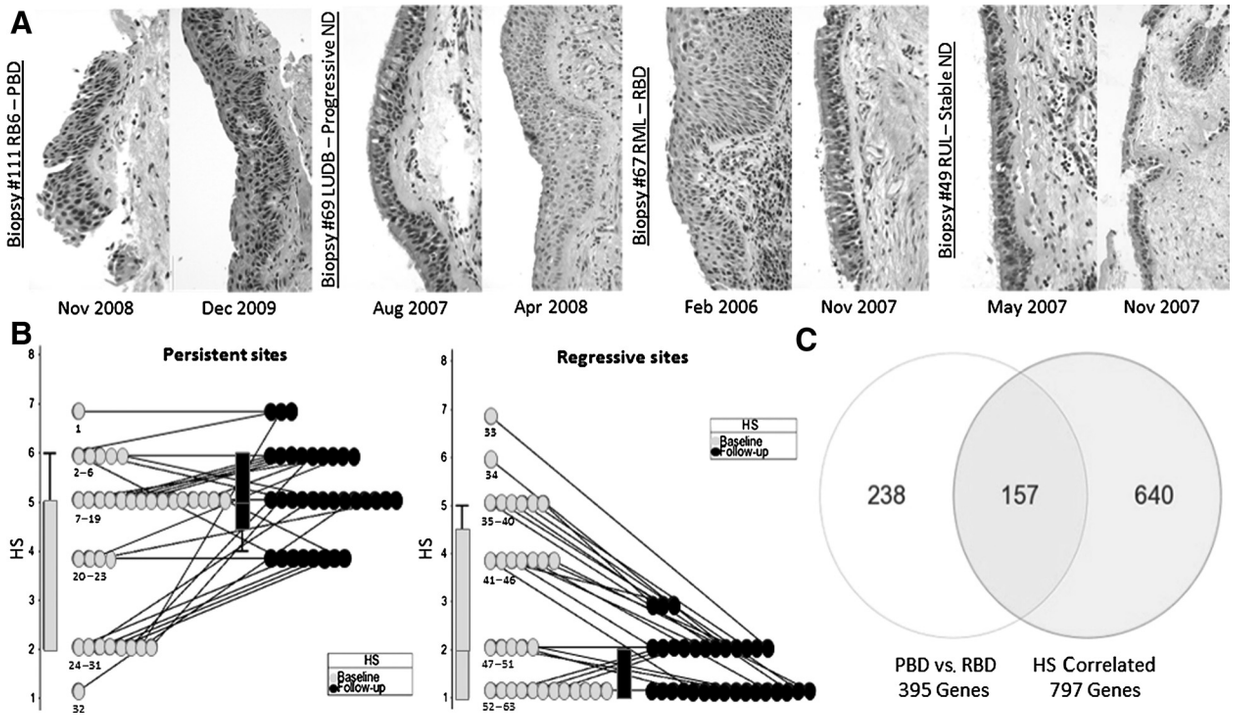

Figure 1.

Summary of specimens analyzed and differentially expressed genes identified in persistent versus regressive bronchial dysplasia. **A,** Representative H&E images (×400) from each of the four classifications of biopsy sites according to baseline and follow-up histology scores at a specific site (ND, nondysplasia). **B,** Graphical representation of all sites included in gene expression analysis comparing persistent (left) and regressive (right) sites. Lines connect baseline (gray dots) and follow-up (black dots) HSs (1 = normal, 2 = reserve cell hyperplasia, 3 = squamous metaplasia without atypia, 4 = mild bronchial dysplasia, 5 = moderate dysplasia, 6 = severe dysplasia, and 7 = carcinoma *in situ*) for consecutive biopsies from a single site within the airway of an individual. **C,** Venn diagram showing overlap of genes that distinguish persistent from regressive sites (light gray circle) and those associated with HS regardless of outcome (dark gray circle).

cell lysates (15–25 μg/lane) from regressive and persistent primary, nonimmortalized dysplastic cell lines at 60% to 90% confluence were analyzed by standard Western blotting procedures using the Li-Core system. These cultures were also grown to near confluence (80%–90% confluent) and either harvested for collection of RNA (RNeasy) or treated with vehicle alone (DMSO, Sigma) or vehicle plus 100 nmol/L Polo-like kinase 1 (PLK1) inhibitor (Volasertib, Selleck) for 48 to 96 hours. Parallel cultures were performed in triplicate with one set each used to measure apoptosis via caspase-3/7 activity (ApoTox-Glo, Promega), cell count by manual cytometer, and cell-cycle fraction via flow cytometric analysis (University of Colorado Flow Cytometry Core). PLK1 expression levels were measured in TaqMan real-time quantitative PCR analyses using validated QuantiTect Primer and SYBR Green PCR mix based assays for PLK1 and GAPDH (Qiagen).

IHC and immunofluorescent staining

Pre-cut slides with 4 to 8 five-micron sections of bronchial biopsy tissue from the Colorado SPORE in Lung Cancer tissue bank were obtained from persistent or regressive sites. Antigen retrieval was performed in citric acid buffer, pH 6.0 (pH 9.0 for PLK1/Cytokeratin), under pressure for 15 minutes to prepare for overnight incubation at 4°C with primary antibodies (IHC/IF) for CD3 (Ventana-2GV6), CD4 (Ventana-SP35/Abcam-EPR6855), CD8 (Ventana-SP57), CD68 (Ventana-KP-1/Abcam-KP-1), HLA-DRA (Abcam-TAL15B), CD206 (Novus-EPR6828(B)), FoxP3 (Abcam-236A-E7), Junctional plakoglobin (PG; Fitzgerald-PG 5.1), Desmoglein 3 (AbD Serotec-5G11), PLK1 (Cell Signaling Technology-208G4), and Pan-keratin (Thermo Fisher Scientific-AE1/AE3). Image annotation was used on IHC-stained slides to demarcate dysplastic epithelial and underlying stromal compartments for image analysis (Aperio, Leica Biosystems) in which percent of positive pixels were used to indicate relative levels of expression in each stained slide. H&E slides for the cases included in this analysis were reviewed prior to inclusion to confirm the presence of appropriate epithelial histology and adequate associated underlying stroma. The mean area of epithelium and stroma analyzed was larger in the group of persistent bronchial dysplasia as compared with the regressive bronchial dysplasias: mean epithelial area 0.139 versus 0.061 (minimum 0.006 vs. 0.007 and maximum 1.033 vs. 0.327) mm^2; mean stromal area 0.173 versus 0.103 (minimum 0.008 vs. 0.010 and maximum 0.994 vs. 0.447) mm^2, respectively ($P < 0.01$). Thus, all results were normalized to the measured area scored for each case. The accuracy of the image analysis was confirmed by comparing manual counts of positive cells by two pathologists (D.T. Merrick and M.C. O'Keefe) to the relative levels of positivity as determined by pixel counts to show similar levels of difference in 12 coscored cases. Immuno-scores (I-score) for DSG3 and PG expression were

Published OnlineFirst July 11, 2018; DOI: 10.1158/0008-5472.CAN-17-3822

calculated by manual classification of dysplastic epithelial regions into proportions (percentage) of negative (intensity = 0) to strongly positive (intensity = 3) areas with the I-score calculated by summing the percent area × intensity for each level of intensity. Two scorers (D.T. Merrick and E.J. Donald) scored all stained sections and cases with I-scores that were more than 50 units different between the two scorers (six cases) were reviewed to generate a consensus score. Otherwise mean scores were used in analyses.

Statistical analysis

Gene expression analysis was conducted using Affymetrix Human Gene 1.0 ST microarrays, and analyzed using RMA and ANOVA methods. Significant differences in expression were defined using an FDR cutoff of 0.05% based on a corrected *t* test. The primary comparison of persistent versus regressive bronchial sites used expression data that were normalized to the mean expression level of a given gene across all groups for the baseline HS that each site demonstrated. The genes meeting criteria for significance were further characterized by employing Ingenuity Pathway Analysis (Qiagen) or KEGG Pathway database (GenomeNet) software to identify associations with biological pathways, biological networks, and upstream regulators that are associated with the genes comprising the final gene list. A *P* value of $\leq$0.05 was used to represent statistical significance in these analyses. Raw gene expression levels were also assessed for trends over the range of baseline HSs. Spearman correlation was applied and *r* values of $\geq\pm$0.5 were considered significant. A *P* value of $\leq$0.05 was used to indicate significant evidence of activation or inhibition of upstream regulator activity. An activation *Z*-score was used to rank upstream regulators in respect to degree of activity. Chi-square and Student *t* tests were employed to assess potential differences between study groups in clinical parameters and in analyses of gene expression, cell cycle, apoptosis, and proliferation in cell culture analyses. Validational analyses employ Student *t* tests of gene expression levels from real-time RT-PCR values normalized to GAPDH expression within each of the triplicate measurements for each cell line. For PLK1 expression analyses, two values in regressive bronchial dysplasia–derived cell lines were excluded due to outlier status (more than 20-fold difference from the mean of the other two replicate measures for that cell line). *t* tests included each measurement for each cell line. A *P* value of $\leq$0.05 is considered statistically significant and *P* values of 0.05–0.15 are considered to be a trend.

Results

Gene expression analysis of bronchial biopsy tissue

Sixty-three frozen biopsies were selected for gene expression analyses. Twenty-three sites represented persistent dysplasias with mild dysplasia (HS = 4) or higher HS at baseline and at least mild dysplasia on follow-up biopsy. The follow-up biopsies for this group always showed an HS that was not less than one lower than the baseline score except for one site in which the baseline score was 6 and the follow-up score was 4. This site was included in the persistent group because additional biopsies collected at this site after the initial follow-up showed HSs of 6. Fifteen regressive dysplasias were characterized by an HS of 4 or higher on baseline sampling and nondysplastic HS (normal, HS = 1 or reserve cell hyperplasia, HS = 2) on follow-up biopsy. Nine progressive nondysplasias (baseline HS = 1–2 and follow-up HS $\geq$ 4) and 16 stable nondysplasias (HS = 1–2 on baseline and follow-up biopsy) were also characterized (Fig. 1A). Initial comparisons showed differences in gene expression in histologically comparable baseline biopsies from persistent bronchial dysplasia versus regressive bronchial dysplasia (142 genes, Supplementary Table S2). Although dysplastic biopsies from regressive sites showed fewer than 90 differentially expressed genes compared with histologically distinct stable nondysplastic sites, persistent sites showed more than 8 times this number versus stable nondysplasia (780 genes). In addition, nondysplastic baseline biopsies that progressed to dysplasia showed 221 differentially expressed genes in comparison with stable nondysplastic sites. Given the minimal differences in gene expression between regressive bronchial dysplasia and stable nondysplasia, the final analysis combined groups into those with dysplasia on follow-up (persistent bronchial dysplasia and progressive nondysplasia, referred to as "persistent sites" throughout the article) and compared this group with those with nondysplastic histology on follow-up (regressive bronchial dysplasia and stable nondysplasia, referred to as "regressive sites"; Fig. 1B). The baseline HS of dysplastic sites, baseline HS of nondysplastic sites, time to follow-up biopsy, smoking status, pack year smoking histories, frequency of history of invasive lung cancer, age, gender, and ethnic distribution were not statistically different between these groups, although a higher percentage of current smokers in the persistent group was near statistical significance (Supplementary Table S1, specimen-specific data in Supplementary Table S3). The mean inflammation score was higher in the regressive group (Supplementary Table S1). ANOVA analysis of normalized gene expression levels revealed 395 genes that were differentially expressed between persistent and regressive groups. The subset ($N = 169$) of genes that were associated with altered cellular pathway activity were selected to represent those most strongly correlated with persistence and supervised hierarchical clustering was performed to further confirm the similarity of the groups combined to form the final persistent and regressive two-group comparison. Only 4 cases in the combined persistent ($n = 32$) and 3 in the combined regressive ($n = 31$) groups showed uncharacteristic expression profiles (Supplementary Fig. S1). Compared with regressive sites, 195 of the full gene list were upregulated and 200 downregulated in persistent sites. In addition, levels of gene expression related to the baseline HS regardless of whether sites showed persistence or regression were assessed. Genes were assessed for the presence of an upward or downward trend in expression with increasing HS. Pearson correlation revealed 797 genes that showed a correlation coefficient of $\geq\pm$0.5 across HS 1–7. Forty percent of the differentially expressed genes associated with persistence were also associated with baseline histology (Fig. 1C).

The gene lists were utilized to identify cellular processes that are associated with persistence and degree of histologic atypia via characterization of activity using the Ingenuity Pathway Analysis program (IPA, Ingenuity, Qiagen). Thirty-one of 232 pathways with which the genes could be associated showed statistically significant evidence of altered activity in persistent sites (Fig. 2A; Supplementary Table S4). These pathways mostly represented three general categories of cellular activity. Fourteen of these pathways are directly associated with immune responses and predominantly show downregulation of the genes associated with these activities. Eight of the pathways mediate cell-cycle regulation and proliferative activities that are commonly associated with malignant disease. Five pathways are associated with regulation of

Published OnlineFirst July 11, 2018; DOI: 10.1158/0008-5472.CAN-17-3822

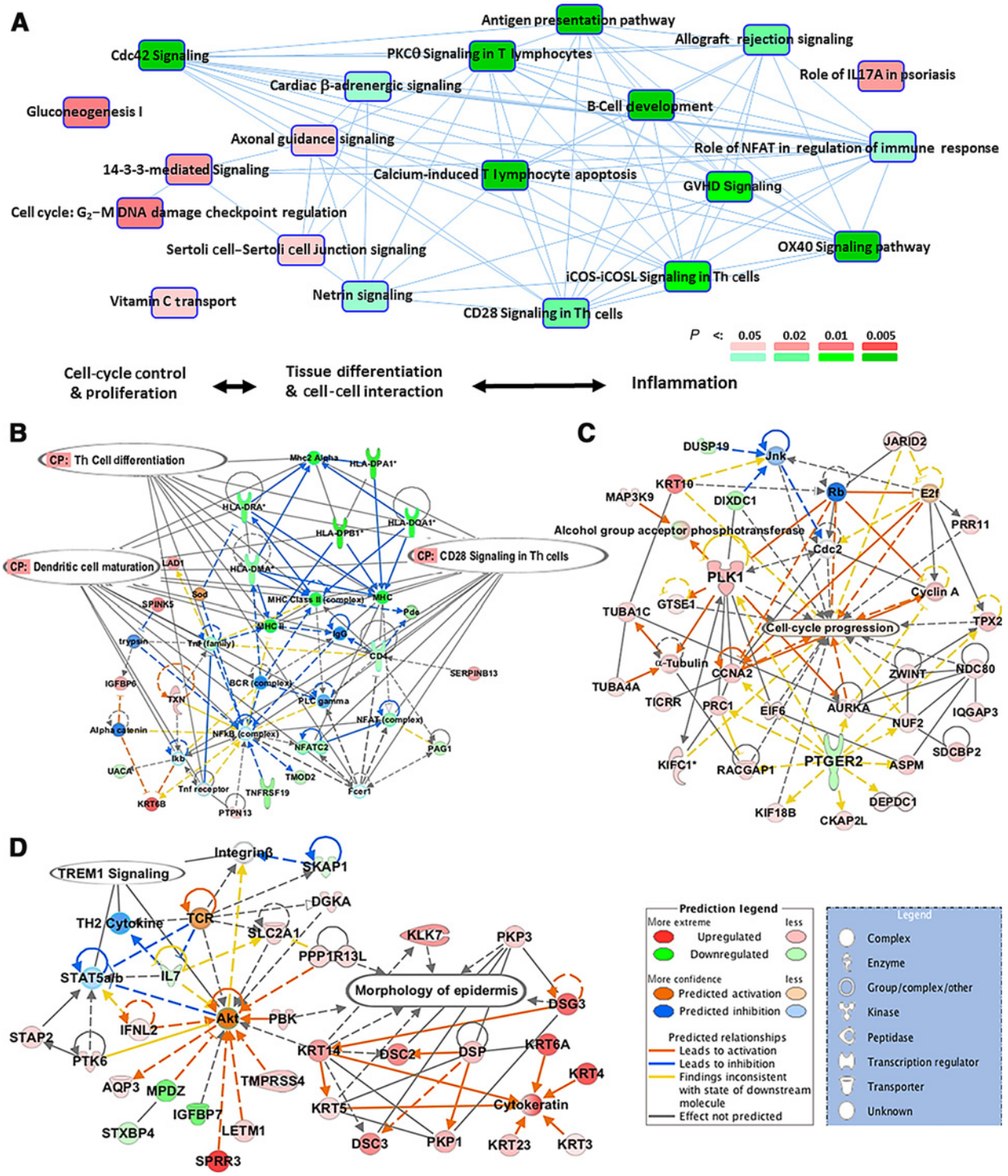

Figure 2.

Pathway and network analyses showing major cellular processes associated with persistence of bronchial dysplasia. **A,** Pathway analysis showing top 20 pathways with significant alteration of activity in persistent versus regressive bronchial dysplasia. Red indicates that the majority of the persistence-related genes associated with a given pathway are upregulated, and green indicates predominant downregulation. Lines connecting pathways indicate that genes are present in both pathways. Intensity of color indicates degree of significance as described in color bar. **B,** Inflammation associated, differentially expressed genes are predominantly downregulated and are strongly associated with Th lymphocyte and dendritic cell networks. **C,** The majority of cell-cycle progression network–associated genes are upregulated and PLK1 shows the most numerous regulatory interactions. **D,** The majority of morphology of epidermis network–associated genes are upregulated and include a number of keratins and desmosomal (desmoglein, desmocollins, plakins) genes.

Published OnlineFirst July 11, 2018; DOI: 10.1158/0008-5472.CAN-17-3822

tissue development encompassing a number of genes that mediate epithelial tissue differentiation, cell–cell interactions, and cytoskeleton-related signaling. The cell cycle and tissue development groups show more frequent upregulation of pathway activity. Pathway analysis utilizing the list of genes associated with baseline histology show that 44 of 261 pathways demonstrate statistically significant evidence of altered activity. Eighteen of the top 22 pathways and 26 overall represent proliferation-associated pathways that are commonly related to cancer development (Supplementary Table S5). Cell-cycle regulation, frequently via pathways coordinating cell-cycle progression with DNA damage responses, is strongly represented. Relatively few pathways (three each) are associated with immune responses and tissue differentiation. Several pathways representing altered metabolic activity and response to cellular injury are correlated with HS. All but four of the histology-related pathways are associated with predominantly up-regulated genes. In addition, the persistence and baseline histology gene lists were used for IPA upstream regulator analysis in which the groups of genes whose expression are known to be regulated by certain signaling proteins are identified and used to indicate significant increases or decreases in signaling by the related upstream regulatory protein. The upstream regulators with the highest positive activation *Z*-scores to be associated with baseline histology were VEGF and β-estradiol (Supplementary Table S6A). VEGF was also the highest to be associated with persistence (Supplementary Table S6B).

Network analyses provided a broader method by which interactions between genes that are differentially expressed in comparisons of persistent and regressive bronchial dysplasia could be assessed. These analyses revealed networks significantly associated with persistence of bronchial dysplasia that were reviewed to further focus the cellular processes we chose to study in the validational analyses presented below. Inflammatory networks associated with persistence were generally downregulated and showed a strong association with helper T-lymphocyte differentiation and macrophage/dendritic cell function networks (Fig. 2B). The cell-cycle progression network included genes that consistently demonstrated upregulation with persistence and identified PLK1 as the central mediator of these activities (Fig. 2C). The morphology of epidermis network demonstrated that most differentially expressed genes were upregulated and identified a number of genes associated with squamous differentiation and desmosomal functions (Fig. 2D).

PLK1 expression and activity are increased in persistent as compared with regressive bronchial dysplasia

PLK1 is the central mediator of activity in three of the top 10 pathways most significantly associated with both persistence and baseline histology. To validate this relationship, PLK1 expression was correlated with increased H-score on follow-up biopsy in the Affymetrix gene expression dataset (Fig. 3A), and high expression in persistent bronchial dysplasia was also demonstrated *in situ* by dual immunofluorescence (Fig. 3B). Expression levels of PLK1 were further assessed in primary cultures of bronchial epithelial cells derived from fresh biopsy tissue. Quantitative real-time PCR-based expression levels were normalized to expression levels of PLK1 in a primary cell line derived from a site showing normal histology over multiple time points. Triplicate measurements in each of two independent studies of PLK1 mRNA levels demonstrated higher mean levels of PLK1 expression in a group of cultures derived from eight persistent bronchial dysplasia sites as compared with measurements from six cultures of regressive bronchial dysplasia. Results from a representative analysis are shown in Fig. 3C, where the mean normalized level of PLK1 expression for persistent bronchial dysplasia was more than twice that of regressive bronchial dysplasia (2.33 vs. 0.88, $P = 0.002$). The majority of the persistent bronchial dysplasia–derived cultures displayed PLK1 RNA levels that were above the mean for regressive bronchial dysplasia. PLK1 protein expression was also found to be elevated in cultured persistent bronchial dysplasia versus cultured regressive bronchial dysplasia by Western blot analysis (Fig. 3D).

SCC of the lung demonstrates one of the highest rates of mutational damage of all malignancies (20). We therefore hypothesized that the role of PLK1 activity in mediating abrogation of cell-cycle arrest in the presence of DNA damage at the G_2–M checkpoint could represent a key cellular alteration associated with progression of bronchial dysplasia to invasive SCC. In addition, effective inhibitors of PLK1 are commercially available and FDA approved for treatment of some malignancies. *In vitro* analyses of the role of PLK1 in mediating cellular proliferation and evasion of apoptotic activity were undertaken to confirm increased PLK1-mediated biological activity in persistent bronchial dysplasia. Treatment with 100 nmol/L of the PLK1 inhibitor volasertib for 3 days led to significant arrest of persistent bronchial dysplasia–derived cells in S–G_2 phase without an impact on cell-cycle progression in normal or regressive bronchial dysplasia (Fig. 4A and B). Similarly, 4 days of treatment with volasertib induced apoptotic activity as measured by caspase-3/7 activity in persistent bronchial dysplasia and to a lesser degree in regressive bronchial dysplasia while not having an effect in cultures of normal bronchial epithelium (Fig. 4C). Volasertib also induced a significant decrease in proliferation in persistent bronchial dysplasia, but did not have a significant effect on proliferation in regressive bronchial dysplasia or normal cultures (Fig. 4C).

Inflammatory responses are downregulated in persistent bronchial dysplasia

Persistence-associated inflammatory pathways indicate significant downregulation in expression of genes associated with macrophage and T-lymphocyte (T-LC) activity in persistent as compared with regressive bronchial dysplasia. Given these observations, inflammation scores that are generated for all biopsies at the time of initial pathologic characterization were used to determine whether there is a difference in overall levels of inflammation related to persistence/regression. Figure 5A shows that the presence of an inflammatory infiltrate was more frequent at sites that showed regressive, nondysplastic histology than those with persistent, dysplastic histology in follow-up biopsies. To determine whether these gene expression changes correlated with actual levels of inflammatory cell types in tissue, numbers of macrophages and T-LCs were assessed in an independent set of 46 persistent and 39 regressive dysplasias by IHC stains for CD68, CD3, CD4, and CD8. The persistent and regressive bronchial dysplasia groups were selected to be matched in respect to inflammation score (mean scores 0.88 vs. 0.83, respectively, $P = 0.77$) and proportion of cases with high-grade inflammation (inflammation scores 2–3; 16.3% vs. 23.1% respectively, $P = 0.44$), as well as age, gender, tobacco status, pack year smoking history, and history of lung cancer (Supplementary Table S7). Image analysis showed a near significant trend toward decreased overall CD68 positivity per area in persistent versus regressive

Published OnlineFirst July 11, 2018; DOI: 10.1158/0008-5472.CAN-17-3822

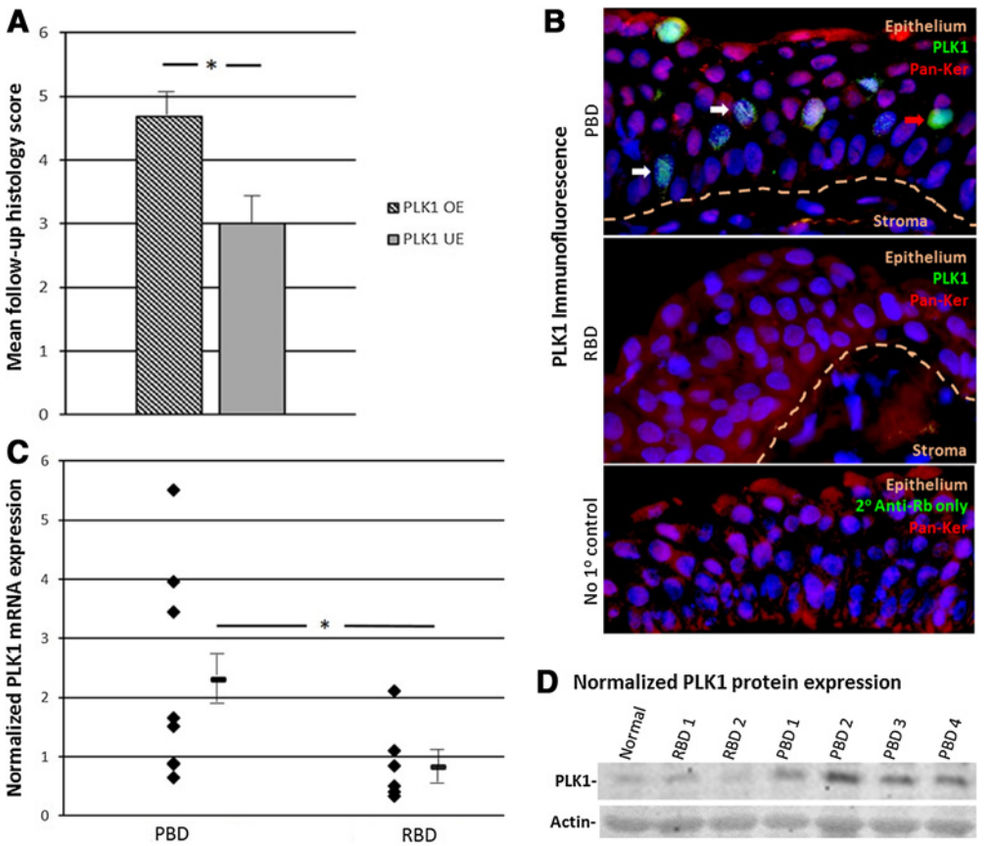

Figure 3.

PLK1 overexpression is associated with persistence of bronchial dysplasia. **A,** Biopsy sites with PLK1 overexpression (PLK1 OE) show higher histology scores in follow-up biopsies than those with underexpression (PLK1 UE). Baseline HSs were not significantly different between OE and UE groups (PLK1 OE = 5.14; PLK1 UE = 4.75; $P = 0.11$). **B,** PLK1/Pan-keratin (Pan-Ker) dual immunofluorescence showing representative frequent moderate (i.e., white arrows) and strong (i.e., red arrow) nuclear and cytoplasmic positivity for PLK1 in persistent bronchial dysplasia (PBD) that is not seen in regressive bronchial dysplasia (RBD). Magnification, ×600. **C,** Cultures of persistent bronchial dysplasia show higher PLK1 expression than regressive bronchial dysplasia. Diamonds, mean of triplicate measurements of a single cell line. Horizontal bars, PLK1 level for the entire group. Vertical bars, SEM (based on all included replicates). **D,** Western blot analysis of PLK1 on protein lysates from normal, regressive bronchial dysplasia, and persistent bronchial dysplasia–derived cultured cells. By densitometry of duplicates from each case, persistent bronchial dysplasia shows increased PLK1 levels versus regressive bronchial dysplasia (normalized mean 1.93 vs. 0.99; $P = 0.02$). Student t test, *, $P < 0.01$.

bronchial dysplasia and similar lower magnitude nonsignificant decreases in CD3, CD4, and CD8 (Fig. 5B and C). Although no subanalyses were statistically significant, the same trends were seen when analyses were restricted to only cases with low or high inflammation scores or restricted to the stromal compartment. No changes were observed in the analysis of the epithelial compartment (Supplementary Fig. S2A and S2B). The gene expression data suggest that alterations in the polarization of inflammatory cell types are key characteristics that distinguish persistent and regressive bronchial dysplasia. Direct assessment of the array-based gene expression levels for a variety of genes that have been reported in the literature to be associated with specific polarization states of inflammatory cell subsets were evaluated (21–28). The majority of genes with statistically significant or near significant differences when comparing persistent with regressive bronchial dysplasia showed decreases in M1 macrophage and Th 1 T-lymphocyte markers, whereas 5 of 9 regulatory T lymphocyte markers were increased in persistent bronchial dysplasia (Supplementary Fig. S2C). To investigate these potential differences, dual immunofluorescence stains to demonstrate subsets of inflammatory cells were used in a small set of representative dysplasias. Figure 5D shows an abundance of dual CD68/HLA-DRA–positive M1 macrophages in regressive bronchial dysplasia compared with persistent bronchial dysplasia. In addition, HLA-DRA expression is noted in epithelial cells of regressive bronchial dysplasia, but not that of the persistent bronchial dysplasia. Conversely, regulatory T-lymphocytes represent a larger proportion of T-LCs in representative persistent as compared with regressive bronchial dysplasia (Fig. 5D).

Altered expression of tissue differentiation and cell adhesion molecules distinguish persistent and regressive bronchial dysplasia

Several pathways associated with persistence are related to cell–cell interactions that contribute to epithelial morphology and nuclear signaling stimulated by physical interactions occurring on the external surface of the cell. These Ingenuity pathways are correlated with gene ontology (GO)–related cellular activities

Published OnlineFirst July 11, 2018; DOI: 10.1158/0008-5472.CAN-17-3822

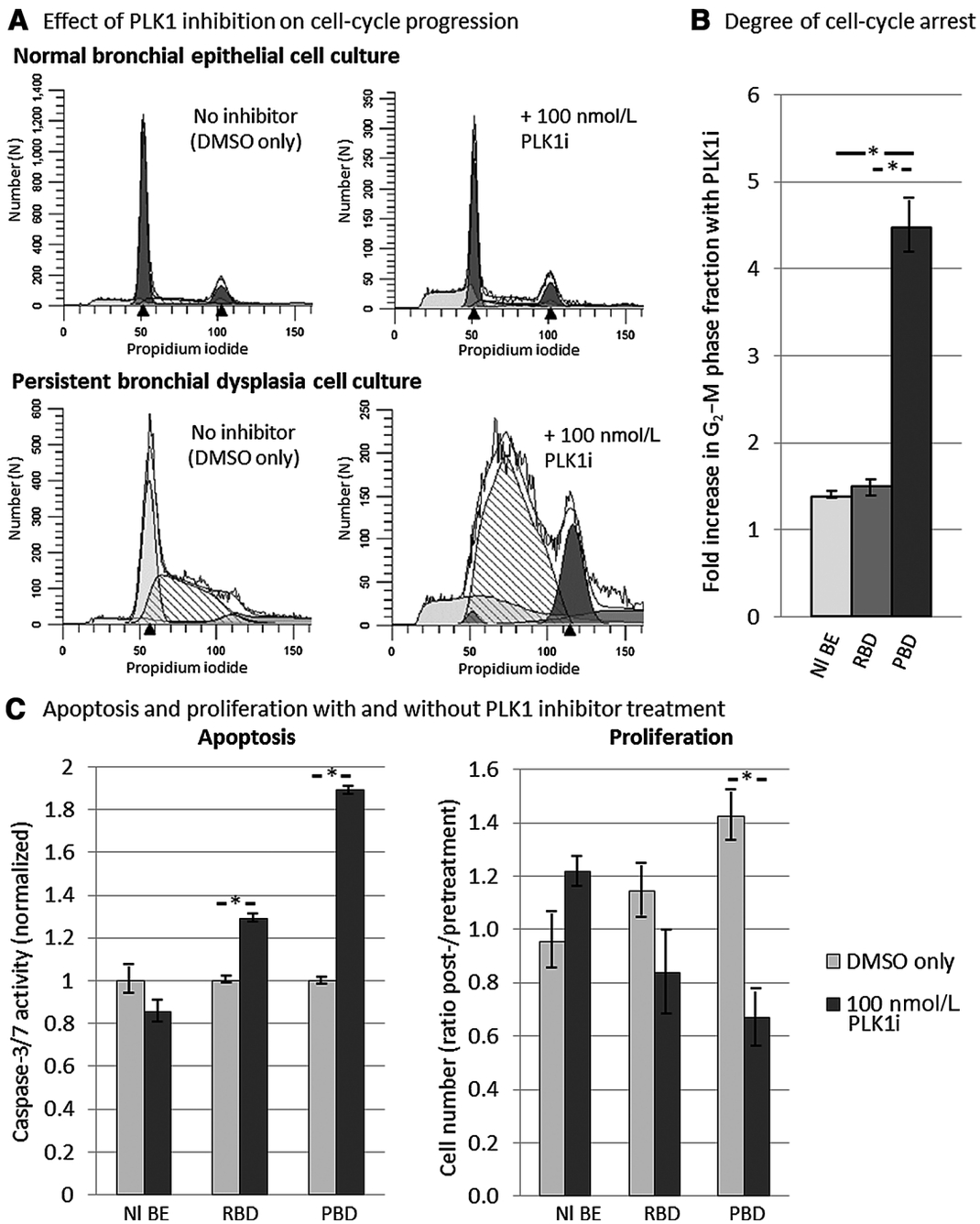

Figure 4.

PLK1 inhibition inhibits cell-cycle progression and induces apoptosis of persistent bronchial dysplasia (PBD). **A,** Flow cytometric analysis of cell-cycle fraction in PLK1 inhibitor, volasertib (PLK1i), treated cultured normal bronchial epithelial (Nl BE), and persistent bronchial dysplasia–derived cells showing an increase in the fraction of cells in the S (diagonal lines) and G_2 (gray peak to the right) phase of the cell cycle in PBD but not normal BE or regressive bronchial dysplasia (RBD)–derived cells. **B,** The proportion of persistent bronchial dysplasia cells arrested at the G_2–M checkpoint is >4-fold higher in PLK1-treated versus vehicle (DMSO) alone–treated cells and significantly greater than that seen in normal and regressive bronchial dysplasia cells (three replicates each of one normal, two regressive bronchial dysplasia, and one persistent bronchial dysplasia cell lines). **C,** Apoptotic activity and inhibition of proliferation are increased in persistent bronchial dysplasia treated with 100 nmol/L but not in normal BE or regressive bronchial dysplasia, although a lesser degree of induction of apoptosis is noted in regressive bronchial dysplasia. Caspase activity is normalized to that measured in vehicle only–treated parallel cultures (16 replicates each of one normal, two regressive bronchial dysplasia, and two persistent bronchial dysplasia cell lines). Cell numbers in analyses of proliferation are expressed as ratios compared with initial seeding of 1×10^5 cells for each cell line/condition (three replicates each). Student *t* test, *, $P < 0.05$.

Published OnlineFirst July 11, 2018; DOI: 10.1158/0008-5472.CAN-17-3822

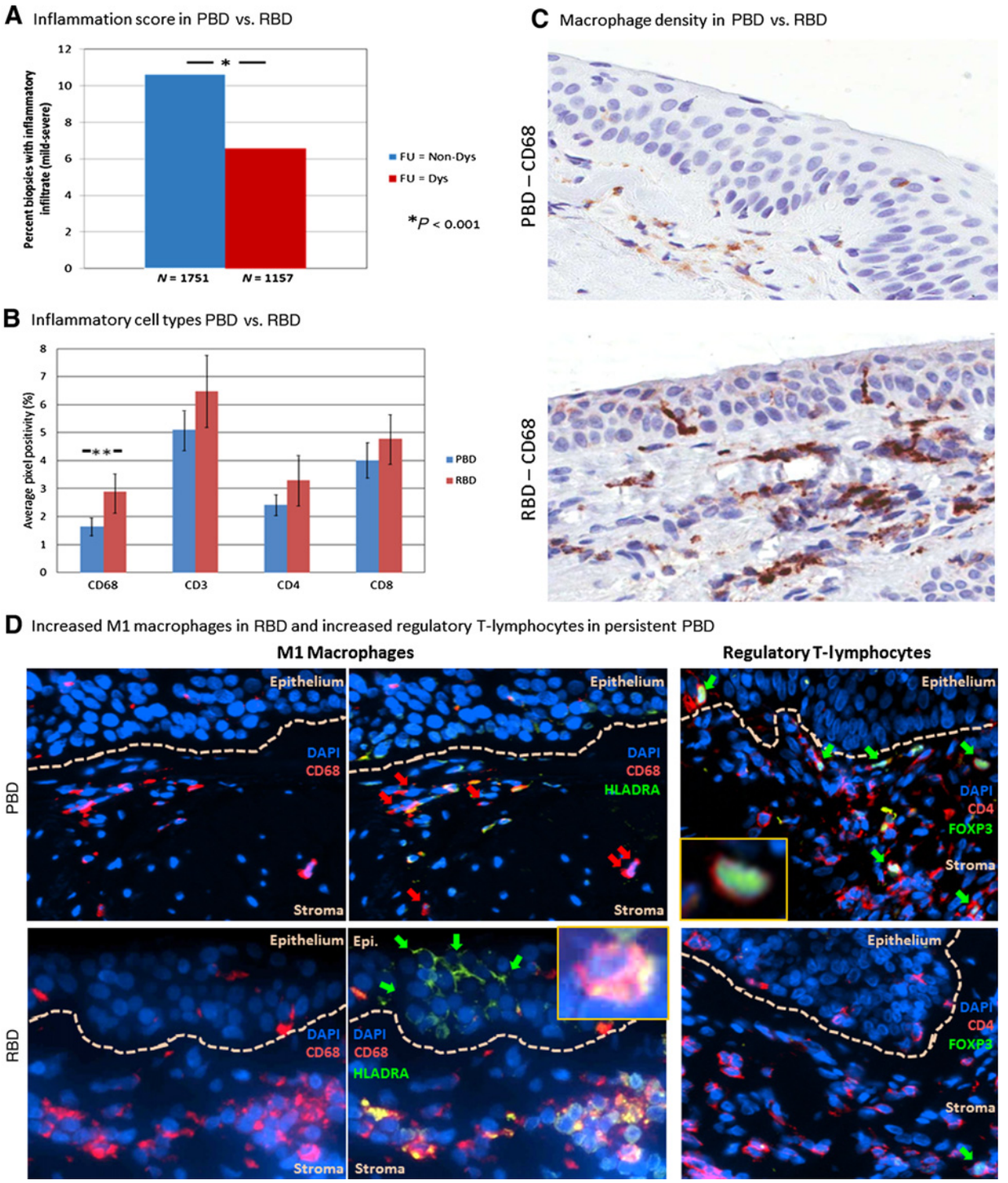

Figure 5.

A, H&E-based mild to severe inflammation scores are more frequent in regressive (RBD) than persistent bronchial dysplasia (PBD). **B,** Macrophage and T-lymphocyte markers are more strongly expressed in regressive than persistent bronchial dysplasia, although only macrophage marker CD68 shows a trend toward statistical significance. **C,** Representative CD68 immunostains. **D,** Dual immunofluorescence stains of representative persistent and regressive bronchial dysplasia. Although the majority of macrophages lack reactivity for M1 marker HLADRA (red arrows, top middle), in regressive bronchial dysplasia, nearly all show dual positivity for CD68 and HLADRA (see inset, bottom middle) and additionally, membranous HLADRA staining is seen in epithelial cells (green arrows). Regulatory T-lymphocytes coexpressing CD4 and FoxP3 (Tregs, green arrows, top and bottom right) are more abundant in persistent as compared with regressive bronchial dysplasia (see inset, top right). Overall, the numbers of M1 macrophages and Tregs in these biopsies were 63.3% (19 dual positive/30 CD68 positive) and 33.7% (28 dual positive/83 CD4 positive) for persistent bronchial dysplasia versus 73.1% (19/26) and 7.0% (4/57) for regressive bronchial dysplasia, respectively. Student *t* test: *, $P < 0.05$; **, $P = 0.05$–0.15.

Published OnlineFirst July 11, 2018; DOI: 10.1158/0008-5472.CAN-17-3822

regulating organismal development emphasizing the potential role of altered gene expression in mediating altered epithelial morphology as demonstrated histologically by the metaplastic change from glandular to squamous epithelium in bronchial dysplasia. Immunofluorescent staining showed that both desmoglein 3 (DSG3) and junctional PG demonstrated predominantly membranous staining patterns (Fig. 6A and B). Immunofluorescence scores (I-scores) based on combined membranous and cytoplasmic staining indicated that high-grade bronchial dysplasia (HGD) demonstrated significantly higher expression of DSG3 than low-grade bronchial dysplasia (LGD) and normal bronchial epithelium while PG showed a trend toward higher expression in LGD as compared with normal bronchial epithelium (Fig. 6C). Persistence of bronchial dysplasia was significantly associated with high expression of DSG3 and showed a trend toward association with PG expression using I-score cutoffs of 50 and 100, respectively (Fig. 6D).

Discussion

Premalignant airway disease precedes the development of invasive SCC, and previously described airway-wide, smoking-related gene expression alterations have recently been shown to predict the presence of dysplastic lesions (29, 30). However, the

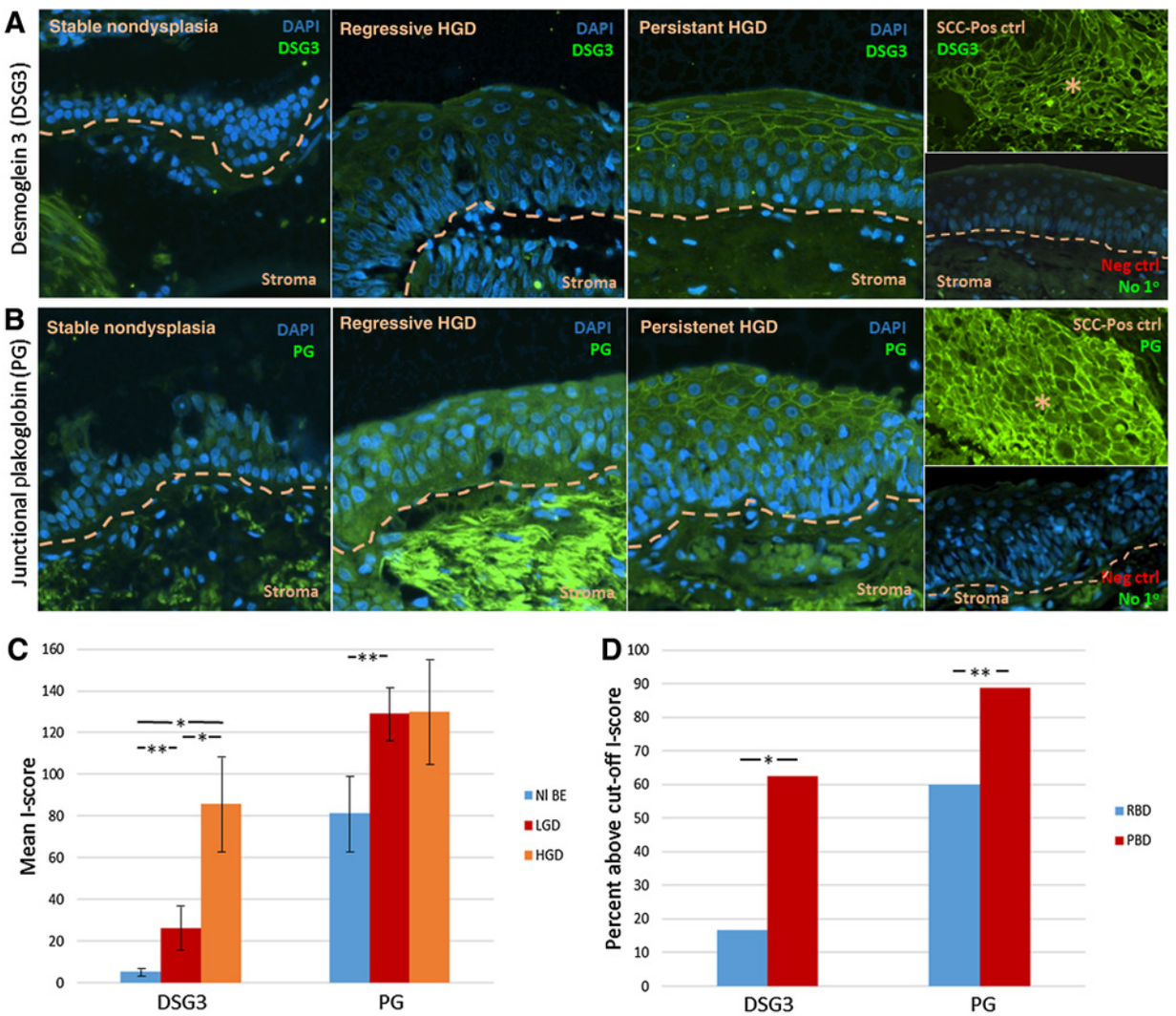

Figure 6.

Expression of desmosomal components is increased in persistent bronchial dysplasia. **A,** Immunofluorescence shows low desmoglein 3 (DSG3) expression in stable reserve cell hyperplasia (left) with increased expression in high-grade regressive bronchial dysplasia (RBD) and strongest expression in high-grade persistent bronchial dysplasia (PBD; right). **B,** A similar pattern of junctional PG expression is noted in stable reserve cell hyperplasia (left) with more pronounced increased expression in high-grade regressive bronchial dysplasia and strongest expression in persistent high-grade bronchial dysplasia (right). Positive controls, invasive skin SCC (DSG3) and lung SCC (PG); negative controls, persistent HGDs with secondary Ab only. **C,** Increased DSG3 expression is seen as histology progresses from normal bronchial epithelium (NI BE; $n = 6$) to LGD ($n = 4$) and HGD ($n = 8$). There is a trend toward increased expression of PG in LGD versus normal BE. Bars, SEM. **D,** More frequent overexpression of DSG3 in persistent ($n = 8$) versus regressive bronchial dysplasia [$n = 12$ (10 for PG)] using an immunofluorescence score (I-score) cutoff of 50 and a trend toward overexpression of PG in persistent bronchial dysplasia using a cutoff score of 100. Magnification, ×200. Student t test (**C**) and χ^2 (**D**): *, $P < 0.05$; **, $P = 0.5$–0.15.

Published OnlineFirst July 11, 2018; DOI: 10.1158/0008-5472.CAN-17-3822

rate of progression to SCC of these lesions is low with even the highest grades only progressing in 5% to 10% of cases (16, 17). Gene expression changes that distinguish high-risk from low-risk bronchial dysplasia have not been reported previously. Herein, we describe gene expression changes associated with the persistent bronchial dysplasias that are characteristic lesions of aggressive airway disease, a condition associated with a 7.8-fold increase in risk for invasive SCC (17). The persistence-associated gene expression profile provides potential markers of risk and indicates alterations in cellular activity that may represent effective targets for prevention of progression to invasive cancer.

Cell-cycle control is prominent in both persistence and dysplastic grade–associated pathways. Although many of the pathways upregulated in association with increasing histologic grade represent DNA damage repair pathways, these pathways are not represented in the comparisons of persistent versus regressive bronchial dysplasia. PLK1 promotes cell-cycle progression and also plays a role in regulating the effect of DNA damage on this progression. PLK1 is required for progression through the M-phase of the cell cycle (reviewed in ref. 31). In addition, PLK1 plays a key role in regulating progression through the G_2–M cell-cycle checkpoint. PLK1 activity can override G_2–M checkpoint arrest in the presence of DNA damage (32–34). In the presence of significant DNA damage, a number of cellular processes will arrest cell cycle–mediated proliferation at this checkpoint and induce apoptosis (reviewed in ref. 35). Our analyses demonstrate an association of PLK1 overexpression with persistence of bronchial dysplasia and show that treatment with PLK1 inhibitor (volasertib, BI6727) arrests persistent dysplastic cells in the S and G_2 phases of the cell cycle while inducing a significant increase in apoptotic activity. These results confirm increased PLK1 activity in persistent bronchial dysplasia and suggest that overexpression may promote genomic instability, leading to the accumulation of somatic genetic damage potentially associated with the development of malignant behavior. The demonstration that the activity of DNA damage repair pathways increases with increasing histologic grade, but that increased activity of these pathways are not specifically associated with high-risk persistent behavior may indicate that although ongoing DNA damage is common in the airways, it is the control of cell-cycle progression that is critical to malignant progression. Indeed, a gene expression study of bronchial dysplasia from four cases of resected invasive SCC showed that one of the characteristics that distinguished the premalignant lesions from normal bronchial epithelium was cell cycle M-phase activation and modulation of microtubule dynamics (36), both processes that PLK1 influences in its role of promoting cell-cycle progression. Thus, our results suggest that PLK1 overexpression could represent a marker of risk for progression and that inhibition of PLK1 may prevent progression of bronchial dysplasia to invasive lung cancer.

Altered activity of inflammatory pathways related to persistence of bronchial dysplasia suggests that influences of the microenvironment play a role in the progression of premalignant airway disease. The data implicate certain specific aspects of broader cellular processes in progression such as the more frequent identification of alterations in cellular than humoral immune responses and the frequent identification of antigen presentation and T-lymphocyte activity in this subgroup of cellular pathways associated with persistence. Intriguingly, the immune response pathways associated with persistence almost exclusively show downregulation of the component genes. Our data show that the presence of an inflammatory infiltrate is more common in regressive than persistent bronchial dysplasia. In lung cancer, a strong general immune infiltrate has been associated with variable but often poor prognosis, although recent studies have clearly established that if the composition of immune cells is oriented toward active responses, such infiltrates can be associated with improved prognosis (37, 38). Potential benefit has been shown when numbers of tumor-associated CD4 and CD8-positive T-LCs or M1 macrophages are increased and adverse effects found when M2-type macrophages or regulatory T-LCs are increased in invasive lung cancers (39, 40). Our analyses suggest that regressive bronchial dysplasia may be associated with decreased regulatory T-LCs and increased antigen presentation capabilities via increased epithelial HLA-DRA expression and the presence of M1-type macrophages, which demonstrate robust antigen presentation and are associated with strong antitumor responses (41). If results from additional studies confirm alterations such as those identified in our pathway analyses, it may suggest that modulation of immune infiltrates could be a successful approach to prevent progression to lung cancer.

Increased expression of DSG3 and PG, proteins associated with desmosomes, indicate alterations of cell–cell interactions and epithelial differentiation in persistent bronchial dysplasia. The structural roles of these factors suggest that increased expression could contribute to squamous metaplastic change that may be more prominent in persistent disease and thus represent potential markers of high-risk bronchial dysplasia. DSG3 is a key component of desmosomes that sequesters prooncogenic desmosomal components associated with epithelial-to-mesenchymal transition, but has recently also been associated with nondesmosomal cytoplasmic activation of protumorigenic SRC signaling (42). Indeed, overexpression of DSG3 has been described in lung cancer and has been associated with poor prognosis in esophageal SCC and pancreatic adenocarcinoma (43–45). PG, a member of the catenin family of proteins, also demonstrates dual activity involving translocation to the nucleus and interaction with transcription factors, although its transcriptional effects have been associated with antioncogenic activities such as inhibition of proliferation, migration, and invasion (46–49). Although some of the immunofluorescence stains did show differences in the distribution of DSG3 and PG (i.e., membranous vs. cytoplasmic/nuclear), the number of cases studied precluded definitive demonstration of differences related to histologic grade or persistence. Further analysis of the factors associated with both up- and downregulation of the cell–cell interaction pathways identified in our gene expression analysis will be required to determine whether alterations in expression of these factors may directly promote protumorigenic activities that could be targeted for prevention.

The gene expression data also show evidence that increased signaling via VEGF and estrogen distinguishes persistent from regressive bronchial dysplasia. Estrogen receptor expression has been associated with poor prognosis in NSCLC, indicating that estrogen signaling contributes to tumor progression (50). Furthermore, administration of estrogen inhibitors in female mice reduced tumor formation providing evidence that estrogen activity may contribute to the development of lung cancer (51). We have previously shown that VEGF and VEGFR2 expression as well as microvessel densities are increased in bronchial dysplasia and invasive lung cancer, especially early-stage tumors, as compared with normal or reactive bronchial epithelium (52). Furthermore, VEGF production by dysplastic epithelial cells

Published OnlineFirst July 11, 2018; DOI: 10.1158/0008-5472.CAN-17-3822

induced endothelial cell proliferation, migration, and tubule elongation (53). A role for VEGF signaling in promoting persistence and progression has also been suggested by observations that bronchial dysplasia showing histologic features of increased angiogenesis (angiogenic squamous dysplasia) demonstrate more frequent persistence and that treatment of mice with vandetanib, a strong inhibitor of VEGFR2, reduced the number and size of urethane-induced tumors (17, 54).

The use of whole biopsy tissue to generate RNA for these studies could represent a drawback as some persistence-related gene expression changes might be masked by RNA derived from nonepithelial cells. In addition, although an extensive set of bronchoscopy-derived specimens are available in the Colorado SPORE tissue bank, the availability of frozen tissue from sites with informative follow-up sampling was limited and thus might also have contributed to false negatives regarding changes in the expression of certain genes. One other recently published study has employed gene expression to assess alterations associated with degree of histologic atypia in precursor lesions of SCC of the lung (55). Unlike our analysis, this study included gene expression from invasive SCCs as part of the spectrum of progression. Nonetheless, similar pathways associated with cell-cycle control and DNA damage repair were also identified, lending support to the validity of the findings in both studies.

To our knowledge, this is the first analysis to describe gene expression alterations that distinguish high-risk from low-risk premalignant SCC precursor lesions. In summary, the identification of a large number of genes that are differentially expressed between histologically indistinguishable lesions lends strong support to the higher risk associated with persistent bronchial dysplasia. Altered activity of pathways associated with these differentially expressed genes shows the importance of cell-cycle regulation, immune infiltrates, and cell–cell interactions in establishing persistent behavior. These findings suggest that markers of these pathways may be useful in predicting which bronchial dysplasias may persist and therefore represent high risk for progression and also facilitate identification of certain cellular activities that might be successfully targeted to prevent the development of invasive cancer.

Disclosure of Potential Conflicts of Interest

No potential conflicts of interest were disclosed.

Authors' Contributions

Conception and design: D.T. Merrick, M.G. Edwards, W.A. Franklin, R.L. Keith, Y.E. Miller, E.J. Donald, G. Hickey, P.A. Bunn, M. Geraci, R.A. Nemenoff

Development of methodology: D.T. Merrick, M.G. Edwards, W.A. Franklin, M. Sugita, R.L. Keith, L.D. Dwyer-Nield, E.J. Donald, A. van Bokhoven, S. Wilson, P.J. Koch, D.J. Orlicky

Acquisition of data (provided animals, acquired and managed patients, provided facilities, etc.): D.T. Merrick, M. Sugita, R.L. Keith, Y.E. Miller, M.B. Friedman, L.D. Dwyer-Nield, M.A. Tennis, M.C. O'Keefe, E.J. Donald, A. van Bokhoven, S. Wilson, P.J. Koch, C. Coldren, D.J. Orlicky, G. Hickey, T.C. Kennedy, R. Powell, M. Geraci

Analysis and interpretation of data (e.g., statistical analysis, biostatistics, computational analysis): D.T. Merrick, M.G. Edwards, L.D. Dwyer-Nield, M.A. Tennis, M.C. O'Keefe, S. Wilson, C. O'Shea, C. Coldren, D.J. Orlicky, X. Lu, A.E. Baron, G. Hickey, P.A. Bunn, M. Geraci

Writing, review, and/or revision of the manuscript: D.T. Merrick, W.A. Franklin, R.L. Keith, Y.E. Miller, L.D. Dwyer-Nield, E.J. Donald, A. van Bokhoven, C. O'Shea, L. Heasley, P.A. Bunn, M. Geraci, R.A. Nemenoff

Administrative, technical, or material support (i.e., reporting or organizing data, constructing databases): D.T. Merrick, E.J. Donald, J.M. Malloy, A. van Bokhoven

Study supervision: D.T. Merrick

Acknowledgments

The authors wish to thank Drs. Aik-Choon Tan and Minjae Yoo for their assistance in creating Supplementary Table S1 and Supplementary Fig. S1, and Elise S. Bales for assistance in performing the immunofluorescence for Fig. 3B. We are grateful to Karen Helm and the University of Colorado Flow Cytometry Core for their guidance and assistance (shared resources supported by P30 CA46934). This work was also supported by Lung Specialized Programs of Research Excellence P50 CA058187, recipients P.A. Bunn and Y. E. Miller (D.T. Merrick, M.G. Edwards, W.A. Franklin, M. Sugito, R.L. Keith, A van Bokhoven, C. Coldren, X. Lu, A.E. Baron, T.C. Kennedy, R. Powell, L. Heasley, P.A. Bunn, M. Geraci, and R.A. Nemenoff), University of Colorado Cancer Center Lung Cancer Prevention Program AWD-120560, recipient D.T. Merrick (M.B. Friedman, L.D. Dwyer-Nield, M.A. Tennis, G. Hickey), Cancer Center Support Grant P30 CA046934, recipient D. Theodorescu (all authors received P30 CA046934 support), Provocative Questions group C-1 R21 CA190124-01, recipient D.T. Merrick (L.D. Dwyer-Nield, M.A. Tennis, E.J. Donald, J.M. Malloy) and Cancer League of Colorado Award, recipient D.T. Merrick (M.C. O'Keefe, E.J. Donald, A. van Bokhoven, S. Wilson).

The costs of publication of this article were defrayed in part by the payment of page charges. This article must therefore be hereby marked *advertisement* in accordance with 18 U.S.C. Section 1734 solely to indicate this fact.

Received December 11, 2017; revised May 16, 2018; accepted July 6, 2018; published first July 11, 2018.

References

1. Siegel R, Naishadham D, Jemal A. (2013) Cancer statistics. CA Cancer J 2013;63:11–30.
2. Zeng C, Wen W, Morgans AK, Pao W, Shu XO, Zheng W. Disparities by race, age, and sex in the improvement of survival for major cancers: results from the National Cancer Institute Surveillance, Epidemiology, and End Results (SEER) program in United States, 1990 to 2010. JAMA Oncol 2015;1:88–96.
3. Aberle DR, Adams AM, Berg CD, Black WC, Clapp JD, Fagerstrom RM, et al. Reduced lung-cancer mortality with low-dose computed tomographic screening. N Engl J Med 2011;365:395–409.
4. Bach PB, Mirkin JN, Oliver TK, Azzoli CG, Berry DA, Brawley OW, et al. Benefits and harms of CT screening for lung cancer: a systematic review. JAMA 2012;307:2418–29.
5. Edell E, Lam S, Pass H, Miller YE, Sutedja T, Kennedy T, et al. Detection and localization of intraepithelial neoplasia and invasive carcinoma using fluorescence-reflectance bronchoscopy: an international, multi-center clinical trial. J Thorac Oncol 2009;4:49–54.
6. Iftikhar IH, Musani AI. Narrow-band imaging bronchoscopy in the detection of premalignant airway lesions: a meta-analysis of diagnostic test accuracy. Ther Adv Respir Dis 2015;9:207–16.
7. Wistuba II, Behrens C, Virmani AK, Mele G, Milchgrub S, Girard L, et al. High resolution chromosome 3p allelotyping of human lung cancer and bronchial epithelium reveals multiple, discontinuous sites of 3pallele loss and three regions of frequent breakpoints. Cancer Res 2000;60:1949–60.
8. Merrick DT, Kittelson J, Winterhalder R, Kotantoulas G, Ingeberg S, Keith RL, et al. Analysis of c-ErbB1/epidermal growth factor receptor and c-ErbB2/HER-2 expression in bronchial dysplasia: evaluation of potential targets for chemoprevention of lung cancer. Clin Cancer Res 2006;12:2281–8.
9. Mascaux C, Laes JF, Anthoine G, Haller A, Ninane V, Burny A, et al. Evolution of microRNA expression during human bronchial squamous carcinogenesis. Eur Respir J 2009;33:352–9.
10. Jonsson S, Varella-Garcia M, Miller Y, Wolf HJ, Byers T, Braudrick S, et al. Chromosomal aneusomy in bronchial high grade lesions is associated with invasive lung cancer. Am J Respir Crit Care Med 2008;177:342–7.
11. Massion P, Zou Y, Uner H, Kiatsimkul P, Wolf HJ, Baron AE, et al. Recurrent genomic gains in preinvasive lesions as a biomarker of risk for lung cancer. PLoS One 2009;4:e5611.

12. Gustafson AM, Soldi R, Anderlind C, Scholand MB, Qian J, Zhang X, et al. Airway PI3K pathway activation is an early and reversible event in lung cancer development. Sci Transl Med 2010;2:1–11.
13. McCaughan F, Pole JCM, Bankier AT, Konfortov BA, Carroll B, Falzon M, et al. Progressive 3q amplification consistently targets SOX2 in preinvasive squamous lung cancer. Am J Resp Crit Care Med 2010;182: 83–91.
14. Breuer RH, Pasic A, Smit EF, van Vliet E, Vonk Noordegraaf A, Risse EJ, et al. The natural course of preneoplastic lesions in bronchial epithelium. Clin Cancer Res 2005;11:537–43.
15. Salaun M, Bota S, Thiberville L. Long-term followup of severe dysplasia and carcinoma in-situ of the bronchus. J Thorac Oncol 2009;4:1187–8.
16. Ishizumi T, McWilliams A, Macaulay C, Gazdar A, Lam S. Natural history of bronchial preinvasive lesions. Cancer Metastasis Rev 2010;29:5–14.
17. Merrick DT, Gao D, Miller YE, Keith RL, Baron AE, Feser W, et al. Persistence of bronchial dysplasia is associated with development of invasive squamous cell carcinoma. Cancer Prev Res 2015;9:96–104.
18. Keith RL, Blatchford PJ, Kittelson J, Minna JD, Kelly K, Massion PP, et al. Oral iloprost improves endobronchial dysplasia in former smokers. Cancer Prev Res 2011;4:793–80.
19. Franklin WA, Folkvord JM, Varella-Garcia M, Kennedy T, Proudfoot S, Cook R, et al. Expansion of bronchial epithelial cell populations by *in vitro* culture of explants from dysplastic and histologically normal sites. Am J Respir Cell Mol Biol 1996;15:297–304.
20. Alexandrov LB, Nik-Zainal S, Wedge DC, Aparicio SAJR, Behjati S, Biankin AV, et al. Signatures of mutational processes in human cancer. Nature 2013;500:415–21.
21. Schmeider A, Michel J, Schonharr K, Goerdt S, Schledzewski K. Differentiation and gene expression profile of tumor associated macrophages. Semin Cancer Biol 2012;22:289–97.
22. Biswas SK, Mantovan A. Macrophage plasticity and interaction with lymphocyte subsets: cancer as a paradigm. Nat Immunol 2010;11:889–96.
23. Heusinkveld M, van der Burg SH. Identification and manipulation of tumor associated macrophages in human cancers. J Transl Med 2011;9: 216–28.
24. Tripathi SK, Lahesmaa R. ranscriptional and epigenetic regulation of T-helper lineage specification. Immunol Rev 2014;261:62–83.
25. Wei G, Abraham BJ, Yagi R, Jothi R, Cui K, Sharma S, et al. Genome-wide analyses of transcription factor GATA3-mediated gene regulation in distinct T cell type. Immunity 2011;35:299–311.
26. Horiuchi S, Onodera A, Hosokawa H, Watanabe Y, Tanaka T, Sugano S, et al. Genome-wide analysis reveals unique regulation of transcription of Th2-specific genes by GATA3. J Immunol 2011;186:6378–89.
27. Cao W, Chen Y, Alkan S, Subramaniam A, Long F, Liu H, et al. Human T helper (Th) cell lineage commitment is not directly linked to the secretion of IFN-c or IL-4: Characterization of Th cells isolated by FACS based on IFN-c and IL-4 secretion. Eur J Immunol 2005;35:2709–17.
28. Smeets RL, Fleuren WWM, He X, Vink PM, Wijnands F, Gorecka M, et al. Molecular pathway profiling of T lymphocyte signal transduction pathways; Th1 and Th2 genomic fingerprints are defined by TCR and CD28-mediated signaling. BMC Immunol 2012;13:1–17.
29. Spira A, Beane JE, Shah V, Steiling K, Liu G, Schembri F, et al. Airway epithelial gene expression in the diagnostic evaluation of smokers with suspect lung cancer. Nat Med 2007;13:361–6
30. Beane J, Mazzilli SA, Tassinari AM, Liu G, Zhang X, Liu H, et al. Detecting the presence and progression of premalignant lung lesions via airway gene expression. Clin Cancer Res 2017;23:5091–100.
31. Bruinsma W, Raaijmakers JA, Medema RH. Switching Polo-like kinase-1 on and off in time and space. Trends Biochem Sci 2012;37:534–42.
32. van Vugt MA, Gardino AK, Linding R, Ostheimer GJ, Reinhardt HC, Ong SE, et al. A mitotic phosphorylation feedback network connects Cdk1, Plk1, 53BP1, and Chk2 to inactivate the G2/M DNA damage checkpoint. PLoS Biol 2010;8:e1000287.
33. Yata K, Lloyd J, Maslen S, Bleuyard JY, Skehel M, Smerdon SJ, et al. Plk1 and Chk2 act in concert to regulate Rad51 during DNA double strand break repair. Mol Cell 2012;45:371–83.
34. Mundt KE, Golsteyn RM, Lane HA, Nigg EA. On the regulation and function of human polo-like kinase 1 (PLK1): effects of overexpression on cell cycle progression. Biochem Biophys Res Comm 1997;239:377–85.
35. Roos WP, Kaina B. DNA damage-induced cell death: from specific DNA lesions to the DNA damage response and apoptosis. Cancer Lett 2013;332:237–48.
36. Ooi AT, Gower AC, Zhang KX, Vick JL, Hon L, Nagao B, et al. Molecular profiling of premalignant lesions in lung squamous cell carcinomas identifies mechanisms involved in stepwise carcinogenesis. Cancer Prev Res 2014;7:487–95.
37. Dieu-Nosjean M-C, Antoine M, Danel C, Heudes D, Wislez M, Poulot V, et al. Long-term survival for patients with non-small-cell lung cancer with intratumoral structures. J Clin Oncol 2008;26:4410–7.
38. Wang L, Zhu B, Miaomiao Z, Wang X. Roles of immune microenvironment heterogeneity in therapy-associated biomarkers in lung cancer. Semin Cell Dev Biol 2017;64:90–7.
39. Ma J, Liu L, Che G, Yu N, Dai F, You Z. The M1 form of tumor-associated macrophages in non-small cell lung cancer is positively associated with survival time. BMC Cancer 2010;10:112.
40. Redente EF, Dwyer-Nield LD, Merrick DT, Raina K, Agarwal R, Pao W, et al. Tumor progression stage and anatomical site regulate tumor-associated macrophage and bone marrow-derived monocyte polarization. Am J Pathol 2010;176:2972–85.
41. Solinas G, Germano G, Mantovani A, Allavena P. Tumor-associated macrophages (TAM) as major players of the cancer-related inflammation. J Leukoc Biol 2009;86:1065–73.
42. Wan H, Lin K, Tsang SM, Uttagomol J. Evidence for Dsg3 in regulating signaling by competing with it for binding to caveolin-1. Data Brief 2016;6:124–34.
43. Saaber F, Chen Y, Cui T, Yang L, Mireskandari M, Petersen I. Expression of desmogleins 1–3 and their clinical impacts on human lung cancer. Pathol Res Pract 2015;211:208–13.
44. Fang W-K, Chen B, Xu X-E, Liao L-D, Wu Z-Y, Wu JY, et al. Altered expression and localization of desmoglein 3 in esophageal squamous cell carcinoma. Acta Histochem 2014;116:803–9.
45. Ormanns S, Altendorf-Hofmann A, Jackstadt R, Horst D, Assman G, Zhao Y, et al. Desmogleins as prognostic biomarkers in resected pancreatic ductal adenocarcinoma. Br J Cancer 2015;113:1460–6.
46. Spindler V, Dehner C, Hubner S, Waschke J. Plakoglobin but not desmoplakin regulates keratinocyte cohesion via modulation of p38MAPK signaling. J Invest Dermatol 2014;134:1655–64.
47. Zhurinsky J, Shtutman M, Ben-Ze'ev A. Plakoglobin and beta-catenin: protein interactions, regulation and biological roles. J Cell Sci 2000;113 (Pt 18):3127–39.
48. Aktary Z, Pasdar M. Plakoglobin: role in tumorigenesis and metastasis. Int J Cell Biol 2012;2012:189521.
49. Winn RA, Bremnes RM, Bemis L, Franklin WA, Miller YE, Cool C, et al. gamma-Catenin expression is reduced or absent in a subset of human lung cancers and re-expression inhibits transformed cell growth. Oncogene 2002;21:7497–506.
50. Stabile LP, Dacic S, Land SR, Lenzner DE, Dhir R, Aquafondata M, et al. Combined analysis of estrogen receptor β–1 and progesterone receptor expression identifies lung cancer patients with poor outcome. Clin Cancer Res 2011;17:154–64.
51. Stabile LP, Rothstein ME, Cunningham DE, Land SR, Dacic S, Keohavong P, et al. Prevention of tobacco carcinogen-induced lung cancer in female mice using antiestrogens. Carcinogenesis 2012;33:2181–9.
52. Merrick DT, Haney J, Petrunich S, Sugita M, Miller YE, Keith RL, et al. Overexpression of vascular endothelial growth factor and its receptors in bronchial dysplasia demonstrated by quantitative RT-PCR analysis. Lung Cancer 2005;48:31–45.
53. Merrick DT, Petrunich S, Miller YE, Keith RL, Kennedy TC, Franklin WA. Chapter 10. Characterization of angiogenic activity and identification of mediators in bronchial dysplasia and invasive lung cancer: role of vascular endothelial growth factor and angiopoietins. In: Litchfield JE ed. New Research on Precancerous Lesions. New York, NY: NOVA Science Publishers; 2007. p. 217–43.
54. Karoor V, Le M, Merrick DT, Dempsey EC, Miller YE. VEGFR-2 targeted chemoprevention of murine lung tumors. Cancer Prev Res 2010;3:1141–7.
55. Koper A, Zeef LAH, Joseph L, Kerr K, Gosney J, Lindsay MA, et al. Whole transcriptome analysis of preinvasive and invasive early squamous lung carcinoma in archival laser microdissected samples. Respir Res 2017;18:12.

Cancer Research
The Journal of Cancer Research (1916–1930) | The American Journal of Cancer (1931–1940)

AACR American Association for Cancer Research

Altered Cell-Cycle Control, Inflammation, and Adhesion in High-Risk Persistent Bronchial Dysplasia

Daniel T. Merrick, Michael G. Edwards, Wilbur A. Franklin, et al.

Cancer Res 2018;78:4971-4983. Published OnlineFirst July 11, 2018.